Investigating the Helicity Modulus of Finite-Size XY Spin Lattices

Kiara Carloni
MIT Department of Physics
(Dated: May 21, 2021)

Vortices in the 2D XY model provided one of the first examples of topological defects in materials. I first review the foundational theory of vortex interactions, repeating Kosterlitz and Thouless's energy-entropy argument, calculating how vortices modify the effective interaction between spins, and completing the renormalization group analysis of the effective coupling. I then extend the renormalization group equations to explain the behavior of finite lattices, and perform Monte Carlo simulations of the XY model on finite lattices of sizes up to L = 512. I estimated the critical temperature at $T_c = 0.8967 \pm 0.0012$.

I. INTRODUCTION

The 2D XY model is a simple model that features a vortex unbinding transition describing a change from quasi-long range to no order.The theory of the transition was first suggested by Kosterlitz and Thouless in 1974, and it successfully predicted a measured jump in the density of superfluid helium [6] [8]. It has since then found numerous applications in describing two-dimensional systems such as liquid crystals, Josephson junction arrays, and superconducting fluid films [1]. The theory was the first investigation of the effect of topological defects in materials. Due to its structural simplicity, it forms an excellent starting point for gaining understanding of how the interactions between defects affect system properties.

II. VORTEX CONFIGURATIONS IN THE XY MODEL

The XY model describes two-component spins $\vec{s}$ on a two dimensional square lattice of size L and spacing a. The model is characterized by the nearest-neighbor interaction Hamiltonian

$$-\beta H = -\beta\rho_s \sum_{<i,j>} \vec{s}_i \cdot \vec{s}_j = -\beta\rho_s \sum_{<i,j>} \cos(\theta_i - \theta_j) \quad (1)$$

. In this expression, β is the inverse temperature, θ_i are the angles of the spins relative to some reference direction, and the summation is conducted over nearest-neighbor bonds between spins. The XY model is often used to describe the phase of the wavefunction of thin films of superfluid helium, for which the gradient $\nabla\theta$ is related to the probability current and the velocity field of the superfluid [7]. The other frequently defined parameter is the coupling constant $K = \beta\rho_s$, which is proportional to the inverse temperature.

If the field θ is smoothly varying, then the difference $\theta_i - \theta_j$ between nearest nieghbors is always small, and we can approximate $\cos(\theta_i - \theta_j) = 1 - \frac{1}{2}(\theta_i - \theta_j)^2 + \mathcal{O}((\theta_i - \theta_j)^4)$. This in turn can be re-written in terms of the gradient of θ when we move from discrete to continuous notation:

$$-\beta H = -\beta E_g - \frac{1}{2}\beta\rho_s \int d^2\vec{r}(\nabla\theta)^2 \quad (2)$$

The local minima of the Hamiltonian are configurations of spins that satisfy $\frac{\delta H}{\delta\theta} = 0$, so these configurations satisfy Laplace's equation $\nabla^2\theta(\vec{r}) = 0$ at all but a few isolated points $\vec{r_i}$.What Kosterlitz and Thouless suggested in their 1973 paper [3] was that apart from the uniform ground state and analytic fluctuations around it, the minimum configurations of the XY model could also include vortices at locations $\vec{r_i}$. The first consequence of this idea was the realization that competition between vortex energy and entropy at different temperatures would characterize distinct phases of the XY model.

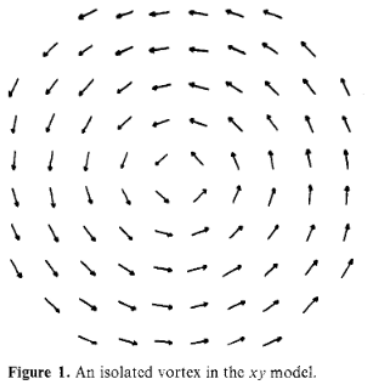

Figure 1. An isolated vortex in the *xy* model.

FIG. 1: A vortex of charge q=1; reproduced from [3]

A vortex such as that in Figure 1 is identified by the property that its contour integral is nonzero: $\oint d\theta_v(\vec{r}) = 2\pi q$ for some integer q; q must be an integer because the angles at the start and ending points must coincide modulo 2π. The integer q is called the winding number or charge of the vortex, and vortices with $q = \pm 1$ are called elementary. The winding number is a topological invariant, and it is impossibleto continuously deform a configuration with given winding number into a configuration with a different one. For this reason, it is not possible to deform a vortex configuration into the uniform ground state.

We can separate the field θ into a potential component θ_{sw} whose contour integral is everywhere zero, and a vortex component θ_v whose contour integrals around points $\vec{r_i}$ are $2\pi q_i$.

Following Kosterlitz's original presentation [4], because θ_v satistifes Laplace's equation we can introduce a conjugate field ϕ such that $\theta_v + i\phi$ is a locally analytic function satisfying the Cauchy-Riemann relations, and use Green's theorem to relate:

$$\begin{aligned}\oint d\theta(\vec{r}) &= 2\pi \sum_i q_i \\ &= \oint (\partial_x \theta_v dx + \partial_y \theta_v dy) = \oint (\partial_y \phi dx - \partial_x \phi dy) \\ &= \iint -(\partial_y^2 \phi + \partial_x^2 \phi) dx dy = \iint -\nabla^2 \phi dV\end{aligned}$$

Thus $\nabla^2\phi(\vec{r}) = -2\pi \sum_i q_i \delta(\vec{r} - \vec{r}_i) = -2\pi n_v(\vec{r})$, and is proportional to vortex distribution function $n_v(\vec{r})$. Using the lattice Laplacian Green's function $G(\vec{r}) = \frac{1}{2\pi}(\ln(R/a) - \ln(|\vec{x}|/a) + c$, [2] ϕ can be written:

$$\begin{aligned}\phi(\vec{r}) &= -2\pi \int d^2\vec{r'} n_v(\vec{r'}) G(\vec{r} - \vec{r'}) \\ &= -\sum_i q_i \delta(\vec{r} - \vec{r}_i) \ln(L/a) + \sum_i q_i \ln(|\vec{r} - \vec{r}_i|/a) + c\end{aligned}$$

The Cauchy-Riemann relations imply that $(\nabla\phi(\vec{r}))^2 = (\nabla\theta_v(\vec{r}))^2$, so using integration by parts, we can express the vortex Hamiltonian:

$$\begin{aligned}-\beta H_v &= -\frac{\beta\rho_s}{2} \int d^2\vec{r} (\nabla\phi)^2 = \frac{\beta\rho_s}{2} \int d^2\vec{r} \phi \nabla^2 \phi \\ &= -\beta \sum_i E_{core} q_i^2 + \beta\rho_s(2\pi) \sum_{i\neq j} q_i q_j \ln(|\vec{r}_i - \vec{r}_j|/a) \\ &\quad - \ln(L/a)(\sum_i q_i)^2\end{aligned}$$

The first term describes the core energy of each vortex, and the second describes a logarithmic interaction between different vortices. The third, however, describes the energy of the total vortex field away from the cores, and grows logarithmically with the system size. Since the configurational entropy of each vortex scales as $S \sim \ln(L^2/a^2)$, the total free energy involves a competition between the logarithmically growing vortex energy and entropy. At low temperatures, a single isolated vortex is energetically prohibited, while at high temperatures, single vortices can proliferate. Charge neutral configurations $\sum_i q_i = 0$ are always much more likely.

The change in system properties between high and low temperature regimes is indicative of a phase transition. In two dimensions, spin wave fluctuations destroy low-temperature long-range order, and spin-spin correlations decay algebraically as $\left\langle \vec{s}(\vec{0}) \cdot \vec{s}(\vec{r}) \right\rangle \approx (a/r)^{(2\pi K)^{-1}}$ [1]. The transition is thus between between a low temperature system with quasi-long range order and a disordered high temperature system.

III. VORTEX INTERACTIONS: RENORMALIZATION GROUP

Vortices reduce the effective coupling constant between spins. Just as internal dipoles shield external charges, leading to a dielectric constant ϵ describing a reduced interaction $C(x)/\epsilon$, internal vortices shield external, yielding an analagous $\epsilon = \frac{K}{K_R}$. The details of the calculation of this interaction for two pairs of elementary vortices are laid out very clearly in [1], section 8.3.

Another way of describing this effect is by calculating how vortices affect the temperature-dependent spin wave stiffness ρ_s^R, defined as the change in the free energy due to an applied gradient. [2] Let $\theta(\vec{x})$ be a set of spin angles describing fluctuations around a spatially uniform state; the spatial average of its gradient is zero. We can apply a gradient by sending $\theta(\vec{x}) \rightarrow \theta(\vec{x}) + \vec{v} \cdot \vec{x}$. The resulting change in the free energy defines the spin-wave stiffness: $F(\vec{v}) - F(0) = \frac{1}{2} V \rho_s^R v^2$. The spin-wave stiffness is also known as the helicity modulus Υ, and, when describing superfluid helium, as the renormalized density.

We can evaluate ρ_s^R to lowest order in v:

$$\begin{aligned}\Delta F(\vec{v}, 0) &= \frac{1}{2} L^2 \rho_s V^2 - T \ln \mathrm{tr} \left[\exp\left[-\frac{\rho_s}{T} \int d^2x v_i u_i \right] \right] \\ &= \frac{1}{2} L^2 \rho_s V^2 \\ &\quad - \frac{\rho_s^2 \beta}{2} \int d^2x d^2x' \left\langle u_i(\vec{x}) u_j(\vec{x'}) \right\rangle v_i v_j + \mathcal{O}(v^4)\end{aligned}$$

The spatial average of the gradient of θ_{sw} was set to zero, so only the vortex portion $\nabla\theta_v$ contributes. Since $\nabla^2\theta_v = 0$, and the system is translation and rotation invariant, the Fourier-transformed correlation can be written

$$\langle \partial_i \theta v(q_1) \partial_j \theta_v(q_2) \rangle = (2\pi^2) \partial^2 (q_1 + q_2)(\delta_{ij} - \hat{q}_i \hat{q}) f(q)$$

for some function f. Then, since $\nabla \times \nabla\theta_v = 2\pi n_v(\vec{x})$, $\partial_j \theta_v = \frac{-i\epsilon_{ji} q_i}{q^2} 2\pi n_v(q)$, and

$$\partial_i \theta_v(q) \partial_i \theta_v(-q) = \frac{1}{q^2} (2\pi)^2 n_v(q) n_v(-q)$$

So we can write ρ_s^R in terms of Fourier-space correlations

of the vortex density:

$$\rho_s^R = \rho_s - \rho_s^2/T \int d^2x \, \langle \partial_i \theta_v(x) \partial_i \theta_v(0) \rangle \tag{3}$$

$$= \rho_s - (2\pi\rho_s)^2/T \lim_{q \to 0} \langle n_v(q) n_v(-q) \rangle / q^2 \tag{4}$$

$$= \rho_s - (2\pi\rho_s)^2/T \lim_{q \to 0} \sum_{i,j} (\vec{r}_i - \vec{r}_j)^2 \langle q_i q_j \rangle \tag{5}$$

In the low temperature regime, the fugacity $y = \exp[-E_{core}/T]$ is small, and the lowest order contribution in y to the vortex charge correlation comes from a single pair of elementary vortices with opposite charge. This results in $\langle q_i q_j \rangle = -2y^2(|\vec{r}_i - \vec{r}_j|/a)^{-2\pi\rho_s/T}$. Dividing by T to relate ρ_s^R to K_R, we finally have

$$K_R = K = -4\pi^3 y^2 \int_a^\infty \frac{dr}{a} (r/a)^{3-2\pi K} \tag{6}$$

The relationship between the renormalized spin wave stiffness ρ_s^R and the effective coupling K_{eff} was argued by analogy here, but can be shown more rigorously by working out the spin correlation function in depth [5] [2]. A renormalization group procedure can be applied to (6) by dividing the integral into two pieces, from a to $e^{\delta\ell}$ and from $ae^{\delta\ell}$ to ∞. The RG flows that result are

$$\begin{cases} \frac{dK^{-1}}{d\ell} & = 4\pi^3 y^2(\ell) + \mathcal{O}(y^4) \\ \frac{dy}{d\ell} & = (2 - \pi K(\ell)) y(\ell) + \mathcal{O}(y^3) \end{cases} \tag{7}$$

The RG procedure effectively coarse-grains over the vortex pairs at smallest separations. This reduces the vortex density, and reduces the effective stiffness, since vortices are screened by hidden pairs. If $K > K_c = \frac{2}{\pi}$, then the RG flows tend towards $y(\ell = \infty) = 0$. This implies that the effective interaction parameter has a square root singularity in T [**?**]:

$$K_e ff = \frac{2}{\pi}(1 - b\frac{2}{\pi}\sqrt{T_c - T} \tag{8}$$

The critical temperature can thus be associated with the largest temperature for which the flow towards $y(\ell = \infty) = 0$ occurs. Since the RG procedure shows that the effective interaction can be written as a function of the renormalization dependent terms $K(\ell), y(\ell)$, taking the limit $\ell \to \infty$ implies $K_R = f(K(\ell = \infty))$, and taking the limit $T \to T_c$ from below results in $K_R^{-1} = \frac{\rho_s^R}{T}$ tending towards $\frac{\pi}{2}$ universally.[6]

IV. FINITE SIZE EFFECTS ON THE HELICITY MODULUS

On a finite lattice, the energy of a single vortex $\tilde{\ln} L$ is finite, and vortices can only interact up to a maximum length scale L. Imposing periodic boundary conditions mimics some aspects of an infinite lattice by strongly discouraging non-neutral vortex configurations, but significant finite-size effects remain. Since the renormalization group flow equations describe how the interactions between and core energies of vortices are adjusted under a change of scale, they also indicate how these parameters are adjusted at finite length scales.

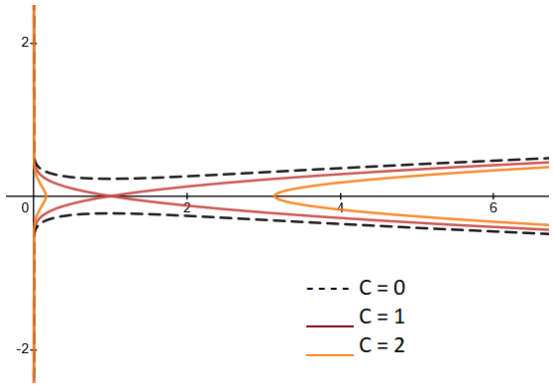

FIG. 2: Solution curves for Eq (9) for C = 0, 1, and 2. Note that at $C = 0$, the curve never intersects the x-axis.

Defining a rescaled coupling constant $x = \frac{2}{\pi}K^{-1}$, the RG equations become $\frac{dx}{d\ell} = 8\pi^2 y^2$, $\frac{dy}{d\ell} = 2(1 - \frac{1}{x})y$, which are solved by the curves

$$x - \ln x - 2\pi^2 y^2 = C \tag{9}$$

for constants C depending on initial conditions. [14] This then means we can rewrite

$$\frac{dx}{d\ell} = 4(x - C - \ln x)$$

. If $K^{-1} = T < \frac{\pi}{2} = T_c$ then in the $\ell \to \infty$ limit, the fugacity y is driven towards zero, and $\frac{dx}{d\ell} = 0$. Thus we can linearize around the fixed point $\bar{x} = x(\ell = \infty)$ satisfying $\bar{x} - C - \ln \bar{x} = 0$. Setting $x = \bar{x} + u$, we have:

$$\frac{du}{d\ell} = 4(u - \frac{u}{\bar{x}} + \frac{u^2}{2\bar{x}}) + \mathcal{O}(u^3)$$

$$\ln(u) = \ln\left(\frac{u}{2\bar{x}^2 + 1 - \frac{1}{\bar{x}}}\right) + 4\ell + c'$$

$$x(\ell, T) = u + \bar{x} = \bar{x}\left(1 + \frac{2(1 - \bar{x})}{1 - c'' \exp\left[-4\ell(1 - \frac{1}{\bar{x}})\right]}\right)$$

The equation (9) has no solutions for $C < 1$, so $C = 1$ must be the constant for the equation at T_c. We can therefore similarly expand $\frac{dx}{d\ell} = 4(x - 1 - \ln x)$ about the fixed point $\bar{x}_c = 1$, resulting in

$$x_c(\ell, T = T_c) = u_c(\ell) + 1 = 1 - \frac{1}{2(\ell + c'')'}$$

The values c'', c''' in the above expressions are constants of integration.

If we identify $e^{\ell} = b$ with the linear system size L, and replace x with $x = \frac{2}{\pi}K^{-1} = \frac{K_c}{K}$, and define $K_\infty(T) = K(L = \infty, T)$ we conclude with:

$$K(L,T)^{-1} = K_\infty(T)^{-1}\left(1 + \frac{2(1 - K_c/K_\infty(T))}{1 - cL^{4K_\infty(T)/K_c - 4}}\right) \tag{10}$$

$$K(L,T_c)^{-1} = K_c^{-1}\left(1 - \frac{1}{2(\ln L + c)}\right) \tag{11}$$

V. MONTE CARLO SIMULATIONS

A. Procedure

I simulated the XY model with the simple Hamiltonian $-H/T = -1/T\sum_{<i,j>}\cos(\theta_i - \theta_j)$, on lattices of sizes $L = 16, 32, 64, 128, 256, 512$ with periodic boundary conditions.

I used the Monte Carlo procedure in order to sample configurations with their associated Boltzmann weight, and I implemented Wolff's cluster algorithm for each Monte Carlo step. This algorithm outperforms the common Metropolis single spin-flip alogirthm near the critical temperature, where its correlation time τ can be a factor of 1000 smaller [10]. At each step, the algorithm picks at random a direction $\hat{n}$ and a seed spin that will form the start of a cluster c. Then the algorithm iterates over the nearest neighbors of each spin added to the cluster c. If two neighboring spins point in the same direction relative to $\hat{n}$, ie. $(\vec{s}_i \cdot \hat{n})(\vec{s}_j \cdot \hat{n}) > 1$, then the neighboring spin is added to the cluster with a proportional probability $P_{\text{add}} = 1 - \exp[-2/T(\vec{s}_i \cdot \hat{n})(\vec{s}_j \cdot \hat{n})]$. At the end of the step, all spins in the cluster are flipped over the line perpendicular to $\hat{n}$. The correlation time per spin is calculated by weighting the Wolff step correlation time by the number of spins in the cluster:

$$\tau = \tau_{\text{steps}}\frac{\langle c\rangle}{L^2} \tag{12}$$

I iniated all models with a random configuration of spins, and prior to taking measurements, I allowed all models to thermalize by running $100L$ Monte Carlo steps. This procedure ensures that measurements are taken only after each configuration has "cooled down" from its disordered state into a state in the microcanonical ensemble for given temperature. I estimated the number of steps to scale linearly in the lattice size L, (as opposed to quadratically for the Metropolis algorithm) because near the critical temperature, clusters in a 2D spin system will percolate, and thus contain on the order of L spins. 100 L Monte Carlo steps should thus be approximately equivalent to 100 full sweeps of the lattice, and sufficient for all models to reach equilibrium configurations.

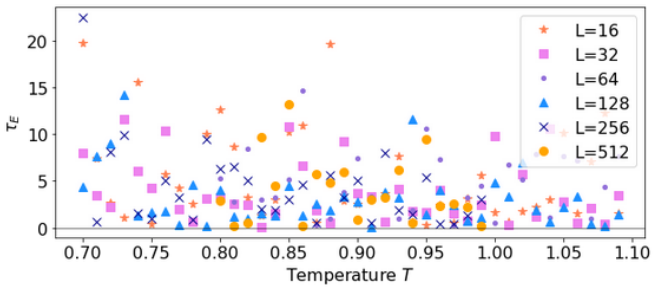

FIG. 3: The correlation time constant τ_E for the calculations of system energy.

I calculated correlation times for each model by weighting the correlation time per step of the configuration energies $\tau_{E\text{step}}$ by the average fractional cluster size as in Eq. (12). The correlation time for an observable O is given by integrating the autocorrelation function χ, which can be calculated for a total number of steps T as [10]:

$$\chi(t) = \frac{1}{T-t}\sum_{t'=0}^{T-t} O(t')O(t'+t) - \frac{1}{T-t}\left(\sum_{t'=0}^{T-t} O(t')\right)\left(\sum_{t'=0}^{T-t} O(t'+t)\right) \tag{13}$$

The resulting correlation times are shown in Figure 3. All the correlation times were $\mathcal{O}(1)$ in L, and correlation effects were neglected in the following calculations.

The helicity modulus $\Upsilon(T) \sim \rho_s(T) \sim J_{\text{eff}}(T)$ can be calculated on a finite lattice by $-\frac{\partial^2 f(v)}{\partial v^2}|_{v=0}$ for a twist $\vec{v} = v\hat{x}$. Then taking two derivatives of $f = \frac{-\ln Z}{L^2}$, with

$$Z = \int d[\theta]\exp\left[-\frac{1}{T}\sum_{<i,j>}\cos(\theta_i + vx_i - \theta_j - vx_j)\right]$$

and setting $v = 0$, gives the helicity modulus as an observable [14]:

$$\Upsilon = \frac{1}{L^2}\left(\left\langle\sum_{<i,j>}\cos(\theta_i - \theta_j)(\hat{x}\cdot\hat{\epsilon}_{ij})\right\rangle - \frac{1}{T}\left\langle\left(\sum_{<i,j>}\sin(\theta_i - \theta_j)\hat{x}\cdot\hat{\epsilon}_{ij}\right)^2\right\rangle\right) \tag{14}$$

The factors $\hat{\epsilon}_{ij}$ indicate the direction of the bonds $i - j$. I evaluated Eq. (14) for each of N recorded Monte Carlo time steps, and then bootstrapped this calculation by selecting a random sample of N values with replacement N times. Bootstrapping replicates the underlying probability distribution for Υ, and thus allows statistical errors to be straightforwardly obtained by measuring the standard deviation [10].

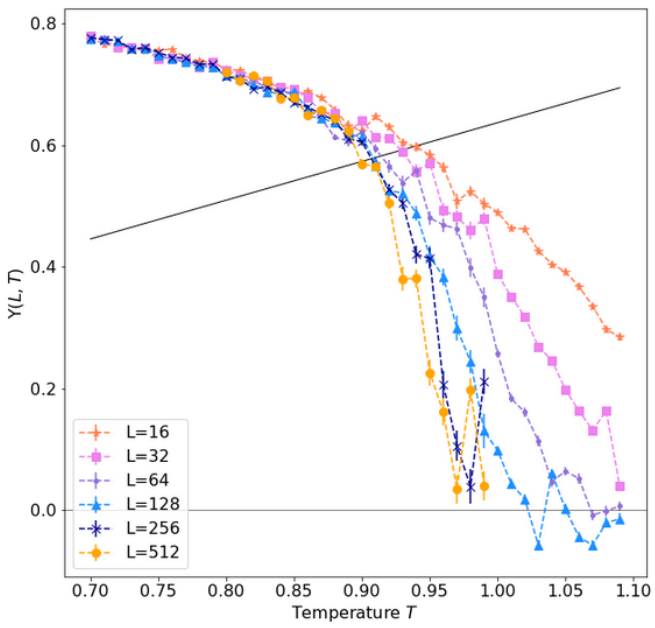

FIG. 4: The helicity modulus Υ, as a function of lattice size L and temperature T. The universal relation $\Upsilon(L,T)/L = \frac{\pi}{2}$ has been plotted in black.

B. Results

Figure 4 shows the resulting plot of the helicity modulus versus temperature at varying lattice sizes. The measured temperatures were chosen to be close to the consensus from previous numerical simulations, $T_c \sim 0.893$ [14][15][16]. For the largest lattice size, $L = 512$, I simulated only temperatures in the narrow range from $T = 0.8$ to the zero Υ point near $T = 0.99$, in order to save on memory space and time costs, while for the other lattice sizes $L = 16, 32, 64, 128, 256$ I simulated from $T = 0.7$ to the zero Υ point near 1.09 or 0.99. Above the critical temperature, the helicity modulus vanishes and finite size effects are more significant. In order to increase statistical precision in this region, I ran 10,000 Monte Carlo steps above $T = 1.0$, and only 1000 below.

The rapid diminishing of the helicity modulus at the critical temperature is clearly visible in Figure 4. Lattice size effects are considerably less significant in the region below the critical temperature, where all four sizes coincide, but are important in determining the location of the critical drop-off. The helicity modulus fluctates about $\Upsilon = 0$ in the region above the critical temperature.

Following the procedure of Schultka and Manousakis in [14], I fitted the resulting $\Upsilon(L)$ for fixed T in the range $(0.8, 0.9)$ to the equation (10), with the integration constant c as a free parameter and $K_c = \frac{2}{\pi}$. Like Schultka and Manousakis, I found that attempting to fit the the equation above the expected critical temperature led to very large uncertainties and poor fits, so I neglected them; the equation was derived under the assumption that $T < T_c$, so this behavior is not unexpected. The results of this fit are listed in table I and shown in figure 5. The fitted values of c vary considerably, suggesting that the fit is not very precise; however, changes to c don't have large effects on the shape of the curve $K(L = \infty, T)$ near the critical temperature. For two values, $T = 0.81$ and $T = 0.87$, the fit in c was very poor and scipy's curvefit function failed to return a covariance matrix for the fit.

T	$K(L=\infty,T)$	c
0.80	1.117 ± 0.003	0.456 ± 0.236
0.81	$1.140 \pm$ n/a	$-1064000 \pm$ n/a
0.82	1.161 ± 0.007	1.027 ± 1.32
0.83	1.190 ± 0.007	1.477 ± 2.26
0.84	1.230 ± 0.006	0.920 ± 0.36
0.85	1.246 ± 0.008	28.950 ± 501
0.86	1.289 ± 0.018	$-3177000 \pm 3.62 \cdot 10^{12}$
0.87	$1.326 \pm$ n/a	$-8852000 \pm$ n/a
0.88	1.392 ± 0.022	1.797 ± 0.96
0.89	1.450 ± 0.020	4.575 ± 7.10

TABLE I: Fitted values of $K(L = \infty)$ for various values of T.

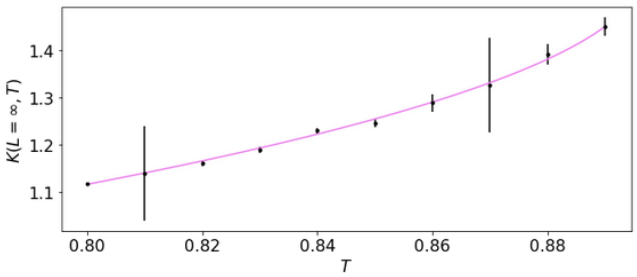

FIG. 5: The fitted values of $K(L = \infty, T)$, and the fitted form (8), with $T_c = 0.8967 \pm 0.0012$, and $b = 0.881 \pm 0.007$. The errorbars for $T = 0.81$ and 0.87 were manually assigned.

I finally fitted the curve $K(L = \infty, T)$, to the scaling form eqrefeq:Keff to get an estimate of the critical temperature at infinite lattice size, $T_c = 0.8967 \pm 0.0012$, which is close to the estimated values by previous works. The constant b was fitted to be 0.881 ± 0.007. Systematic errors, such as insufficient thermalization or missed subleading finite size corrections [16] mean the actual uncertainty on this result is significantly larger than stated.

VI. CONCLUSION

Up to statistical fluctuations, the analytic forms for XY model properties and numerical results coincided. The numerical results could be significantly refined by sam-

pling a larger subset of lattice sizes, and by increasing the number of Monte Carlo measurements recorded. The process of approaching the same quantity $\rho_s^R = \Upsilon$ from multiple points of view expanded my understanding of the applications of the renormalization group procedure, and of how temperature, system size, and interaction strengths affect the configurations of the XY model.

Acknowledgments

Thanks to the 8.334 staff for an excellent semester!

[1] M. Kardar, *Statistical Physics of Fields* (Cambridge University Press, 2007)
[2] P. Chaikin and T. Lubensky, *Principles of Condensed Matter Physics* (Cambridge University Press, 1995)
[3] J. M. Kosterlitz and D. J. Thouless (1973), J. Phys. C: Solid State Phys. 6, 1181
[4] J. M. Kosterlitz (1974), J. Phys. C: Solid State Phys. 7, 1046
[5] J. V. Jose, L. P. Kadanoff, S. Kirkpatrick, R. Nelson (1977), Phys. Rev. B 16, 1217
[6] D. Nelson, J. M. Kosterlitz (1977), Phys. Rev. Lett. 39, 1201
[7] H. J. Jenson, Lecture Notes for Imperial College London
[8] D. J. Bishop and J. D. Reppy (1978), Phys Rev. Lett. 40, 1727
[9] I. Herbut, *A Modern Approach to Critical Phenomena* (Cambridge University Press, 2007)
[10] M. E. J. Newman and G. T. Barkema, *Monte Carlo Methods in Statistical Physics* (Oxford University Press, 2001)
[11] U. Wolff (1988), Phys. Rev. Lett 62, 361
[12] T. Ohta and D. Jasnow (1979) Phys. Rev. B. 20, 139
[13] J. Rudnick and D. Jasnow (1977) Phys. Rev. B. 16, 2032
[14] N. Schultka and E. Manousakis (1993), Phys. Rev. B 49, 12071
[15] P. Olsson (1995) Phys. Rev. B 52, 51
[16] M. Hasenbusch (2005) J. Phys A38, 5869